Extended Abstracts of the 17th Conference on Solid State Devices and Materials, Tokyo, 1985, pp. 57-61

B-1-1

Invited

Enhanced Disordering of AlGaAs Superlattice and its Application to Fabrication of Index-Guided Multiquantum Well Lasers

Hisao Nakashima

Optoelectronics Joint Research Laboratory
Kamikodanaka, Nakahara-ku Kawasaki 211, Japan

Diffusion of Zn or Si into GaAs-AlGaAs superlattices or multiquantum well (MQW) structures promotes the intermixing of Ga and Al, resulting in compositionally disordered AlGaAs. This diffusion-induced disordering (DID) occurs at much lower temperatures than that without impurity diffusion. We briefly review our results on this DID phenomenon and discuss its mechanisms. We also describe the application of DID to the fabrication of index-guided MQW lasers.

§1. Introduction

Laidig et al. have first demonstrated that the diffusion of Zn into AlAs-GaAs superlattices (SL's) dramatically promotes the intermixing of Al and Ga.[1] Similar results have been obtained for Si implantation and subsequent annealing[2] and for Si doping during growth followed by heat treatment.[3] These phenomena have been proposed to be closely related with the diffusion mechanisms of impurities.[4] The relatively low temperature disordering of SL's and multiquantum well (MQW) structures seemed to be detrimental to the fabrication of SL or MQW devices whose characteristics depend largely on the abruptness of heterointerfaces. However, it has been successfully demonstrated that a transverse mode controlled MQW laser, called a buried MQW (BMQW) laser, can be fabricated by Zn-diffusion-induced disordering (Zn-DID).[5,6] Since then, the DID process began to provide new possibilities in the III-V device technology.

In this paper, we present our results on the enhanced disordering of SL's and describe its application to the fabrication of index-guided MQW lasers.

§2. Enhanced Disordering of Superlattices

At relatively high temperatures ($\sim$ 1000°C), thermal annealing leads to disordering of SL's or MQW's.[7~9] Diffusion of Zn or Si induces this disordering at much lower temperatures.[1,2] This DID phenomenon is clearly observed by cross sectional transmission electron microscopy (TEM), as shown in Fig. 1.[10] The sample observed was made by selective diffusion of Zn into an MBE grown MQW structure composed of ten 80 Å GaAs wells separated by nine 60 Å $Al_{0.3}Ga_{0.7}As$ barriers. As can be seen in this TEM micrograph, the GaAs and AlGaAs layers are distinctly observed in black and white layer contrasts, respectively, in the ordered region, while no contrast in the Zn diffused region. This shows that the MQW structure is completely disordered

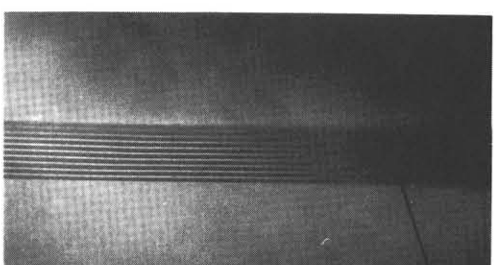

Fig. 1 Cross sectional TEM micrograph of MQW and Zn diffused disordered region.

by Zn diffusion, resulting in uniform AlGaAs with averaged composition. Typically, the Al-Ga interdiffusion constant is $\sim 10^{-18}$ cm^2/sec at 850°C without Zn diffusion,[7] whereas it increases to $\sim 10^{-13}$ cm^2/sec at 575°C with Zn diffusion.[1,11] The narrow transition region less than 0.2 μm is explained by the steep Zn concentration gradient of Zn-diffusion front. This indicates that DID is critically dependent on Zn concentration. The minimum required Zn concentration for DID has been reported to be about 10^{18} cm^{-3}.[11]

Difusion of Zn in GaAs is generally believed to proceed via Zn interstitials (Zn_I) and As vacancy (V_{As}) pairs.[12] It is proposed that those Zn_I and V_{As} are responsible for the DID process.[4] The proposed model shows that the Al-Ga intermixing is induced by V_{As} diffusion by nearest-neighbor hopping, forming the concomitant Zn_I and antisite complexes. However, no clear evidence for V_{As} and antisite defects has been reported, as far as we know. Only Zn_I has been detected by particle-induced X-ray emission (PIXE) in combination with ion channeling.[13]

Si ion implantation and subsequent annealing also induces disordering of SL's. Figures 2 and 3 show sputter Auger profiles for GaAs (300 Å)/ $Al_{0.5}Ga_{0.5}As$ (300 Å) SL's implanted with 80 keV and 160 keV focused Si ion beams and annealed at 850°C for 2 hr. Considering the projected range and standard deviation of Si implanted into AlAs and GaAs, the depth of the disordered region is deeper than expected. Disordering of SL's has been reported to be induced by doping of Si during MBE growth followed by heat treatment[3]

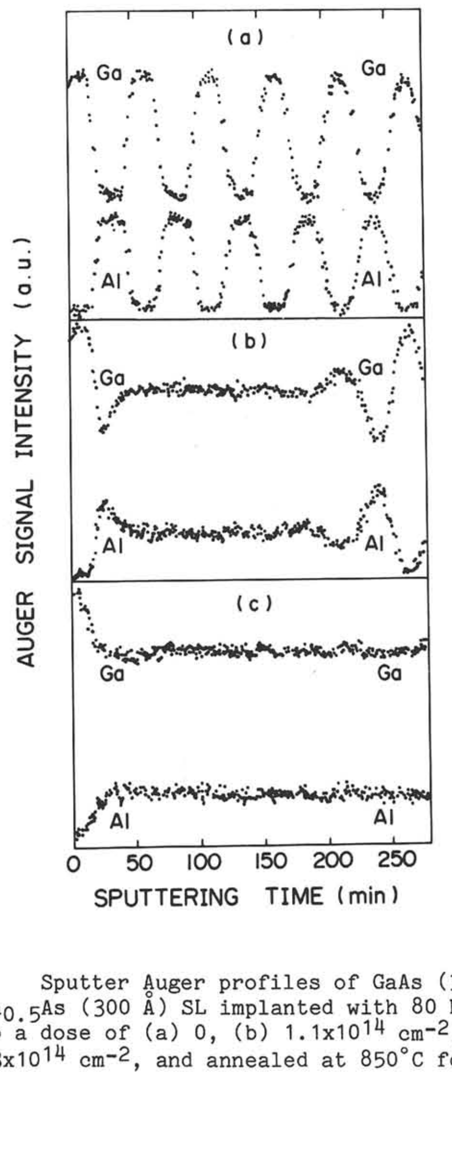

Fig. 2 Sputter Auger profiles of GaAs (300 Å)/ $Al_{0.5}Ga_{0.5}As$ (300 Å) SL implanted with 80 keV Si ions to a dose of (a) 0, (b) $1.1x10^{14}$ cm^{-2}, (c) $2.3x10^{14}$ cm^{-2}, and annealed at 850°C for 2 hr.

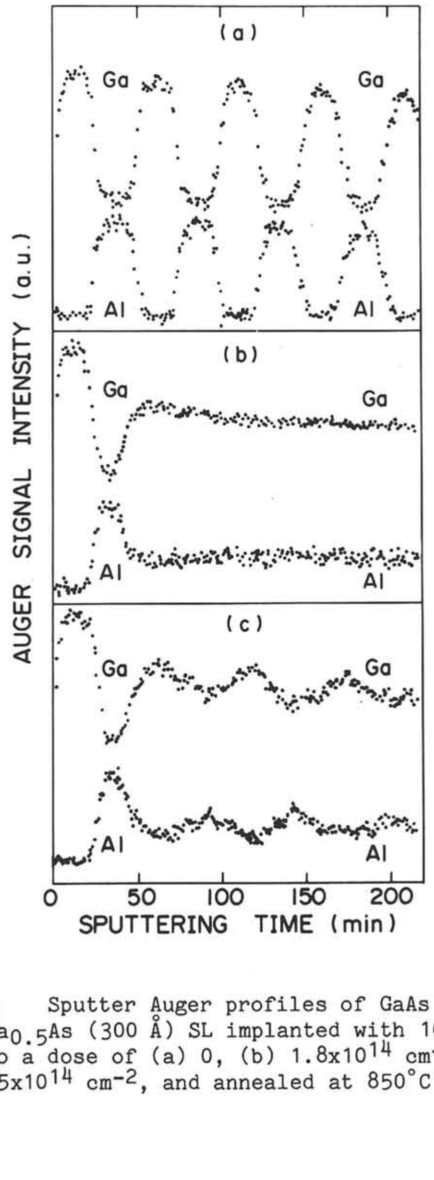

Fig. 3 Sputter Auger profiles of GaAs (300 Å)/ $Al_{0.5}Ga_{0.5}As$ (300 Å) SL implanted with 160 keV Si ions to a dose of (a) 0, (b) $1.8x10^{14}$ cm^{-2}, (c) $4.5x10^{14}$ cm^{-2}, and annealed at 850°C for 2 hr.

and thermal diffusion from evaporated Si films.[14] All these results indicate that diffusion of Si plays an important role in the disordering mechanism. It has been demonstrated that Si diffuses rapidly at high concentration where Si_{Ga}-Si_{As} pairs tend to form.[15] Direct evidence of the Si_{Ga}-Si_{As} pair formation at concentration higher than 1×10^{18} cm^{-3} has been provided by the channeling PIXE measurements.[16] In this case, Si_{Ga}-Si_{As} pairs can move substitutionally by exchanging sites with either V_{Ga} or V_{As} which diffuses in the opposite direction to Si diffusion. This V_{Ga} or V_{As} diffusion seems to cause the Al-Ga intermixing.

The surface top layer where damage is introduced by implantation is never disordered completely, as shown in Figs. 2 and 3. Moreover, as shown in Fig. 3, the complete disordering does not occur at high energy and high dose implantation, which introduces larger amount of damage. These results suggest that the damage introduced by implantation suppresses the Al-Ga intermixing. Si may be trapped by the damage or may diffuse by different mechanism from the above mentioned.

§3. Device Application

Here, we give a few examples of application of DID to the fabrication of MQW lasers. First one is a BMQW laser, which is schematically illustrated in Fig. 4. Zinc was selectively diffused at 630°C for 40 min. into an MBE grown MQW structure, resulting in a 2 ∿ 8 μm wide stripe region. Since the MQW region has a refractive index larger than that for DID region,[17] an optical waveguide was formed by this DID process.

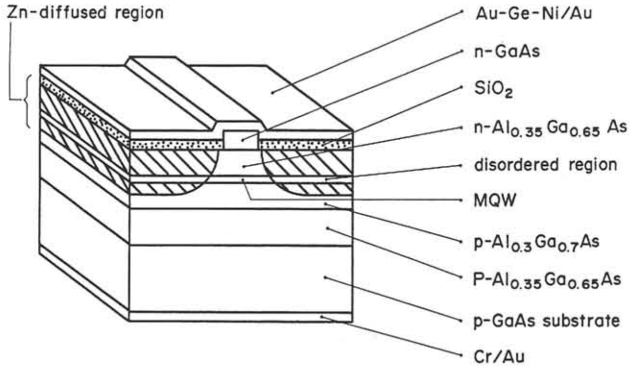

Fig. 4 Schematic illustration of the BMQW laser structure.

Typical pulsed L-I characteristics of BMQW lasers are shown in Fig. 5. The stripe width and cavity length of the lasers are 2.2 μm and 300 μm, respectively. The laser examined were randomly selected from one wafer. The threshold current is typically 20-25 mA, which shows a good wafer uniformity. The maximum light output power is 65 mW/facet and differential quantum efficiency is as high as 75%. The threshold current proportionally increases with the stripe

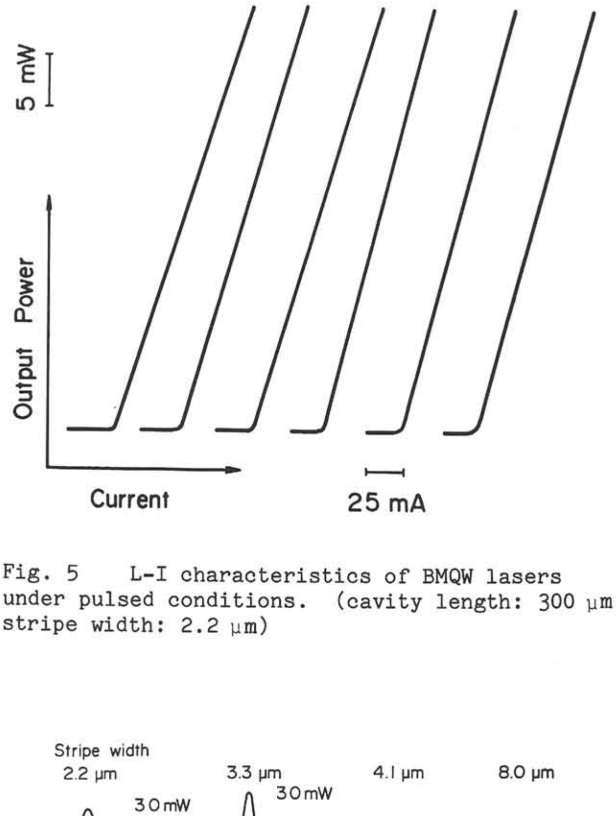

Fig. 5 L-I characteristics of BMQW lasers under pulsed conditions. (cavity length: 300 μm, stripe width: 2.2 μm)

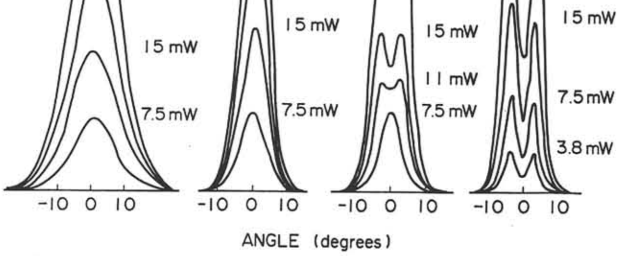

Fig. 6 Far-field patterns parallel to the junction plane of BMQW lasers with various stripe widths.

width. This result togather with the high differential quantum efficiency, which is independent of the stripe width, demonstrates that the BMQW structure provides a small leakage current and extremely good current confinement.

The most eminent feature of a BMQW laser is controllability of the transverse mode. The transverse mode is controlled by controlling the stripe width. Far-field patterns parallel to the junction plane of four lasers with different stripe width are illustrated in Fig. 6. Near-field patterns of lasers with 3 and 7 μm stripe width at different bias currents are shown in Fig. 7 (a) and (b). The laser with narrow stripe width, less than 3.3 μm, operates in the lowest single transverse mode. As usual for an index-guided laser, a single longitudinal mode was obtained, in cw operation, except near the threshold. All these results show that the BMQW laser acts as an index-guided laser.

Next example is a window stripe BMQW laser which is schematically illustrated in Fig. 8. High power operations of semiconductor lasers can be realized by making the laser structure transparent to the laser light in the vicinity of mirrors, which is called a window structure.[18] This window structure was accomplished by selective Zn diffusion which induced disordering of MQW, resulting in a larger bandgap region transparent to the laser light.[19] Combining the window and BMQW structure, transverse mode controlled high power lasers can be realized simply using Zn-DID process.

The maximum pulsed light output of the window stripe BMQW laser was about 240 mW, while it was 130 mW for the BMQW laser without window fabricated from the same wafer.

The far-field patterns for a window stripe BMQW laser showed a stable fundamental transverse mode up to 100 mW. The external differential quantum efficiency and threshold current depended on the total window region length. This is due to the large free carrier absorption in the Zn diffused window region. By controlling diffusion depth and window region length, the window stripe BMQW lasers with low threshold current and high external quantum efficiency were realized.

Another example is an MQW laser with buried MQW optical guide (MQW-BOG)[20], which is shown in Fig. 9. Since the MQW-BOG layer located above the active layer, controls the transverse mode, the optimized MQW structure or the single quantum well is possible for the active region. The pnp current blocking structure outside the stripe as well as MQW-BOG was formed by Zn diffusion.

For the lasers with 3 μm wide stripe and 300 μm long cavity, the threshold currents of 60-80

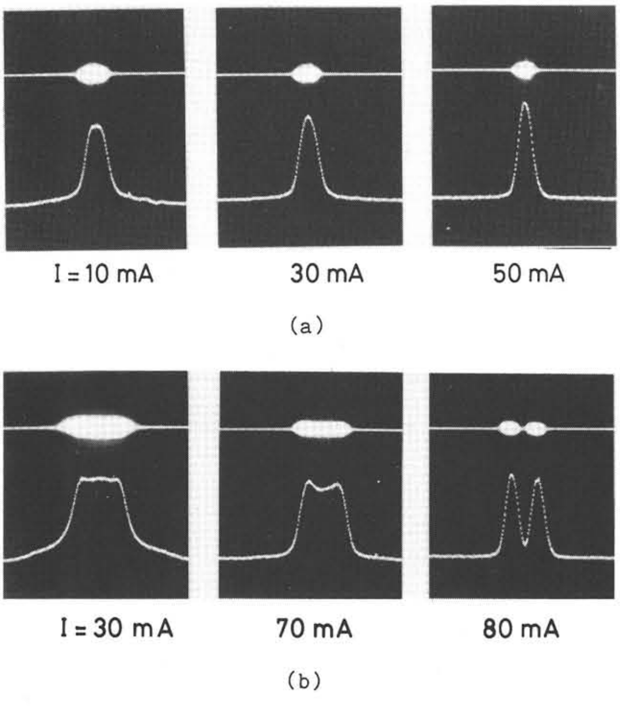

Fig. 7 Near-field patterns of BMQW lasers with (a) 3 μm stripe width and 30 mA threshold current, (b) 7 μm stripe width and 70 mA threshold current at different bias currents. Light intensity profiles were obtained by scanning along the lines indicated in the near-field patterns.

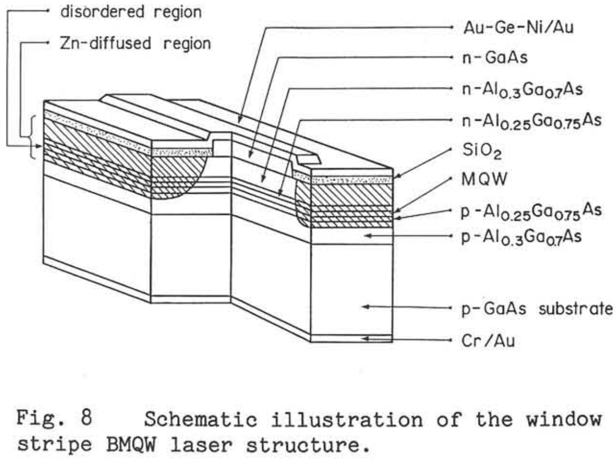

Fig. 8 Schematic illustration of the window stripe BMQW laser structure.

mA were obtained under pulsed conditions. The output power increased linearly with increasing the current up to 30 mW, in the single transverse mode. However, the small kink was observed in the light output vs. current curve over the output power of 30 mW, where a twin peak appeared in the far-field pattern, while a single peak in the near-field pattern. From these results, it is confirmed that the MQW-BOG laser acts as an index-guided laser with partial gain-guided effect.

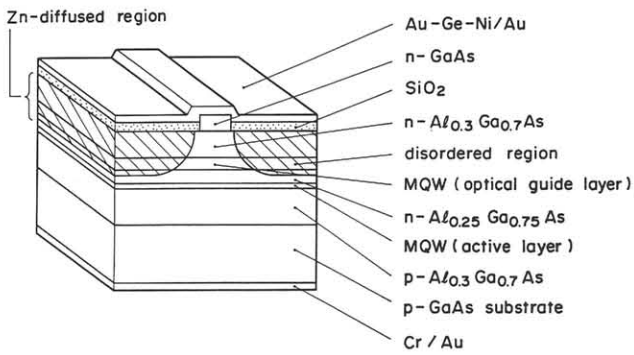

Fig. 9 Schematic illustration of the MQW-BOG laser structure.

§4. Conclusion

As shown in this review, the disordering of SL's is dramatically induced by impurity diffusion. This DID process has been applied to the fabrication of index-guided MQW lasers. Although the DID process has many possibilities for practical application, its mechanism is not clear. Both experimental and theoritical studies will be needed to clarify the elemental processes of this DID phenomenon.

Acknowledgement

Auther would like to thank Drs. K. Ishida, T. Fukunaga, S. Semura, T. Ohta, T. Kuroda, Y. Uchida T. Narusawa, K. L. I. Kobayashi, E. Miyauchi, and H. Hashimoto for their collaboration.

The present researches are part of the large-scale project "Optical measurement and control systems", conducted under a program set up by Agency of Industrial Science and Technology, the Ministry of International Trade and Industry.

References

1) W. D. Laidig, N. Holonyak, Jr., M. D. Camras, K. Hess, J. J. Coleman, P. D. Dapkus, and J. Bardeen, Appl. Phys. Lett. 38, 776 (1981)
2) J. J. Coleman, P. D. Dapkus, C. G. Kirkpatrick, M. D. Camras, and N. Holonyak, Jr., Appl. Phys. Lett. 40, 904 (1982)
3) M. Kawabe, N. Matsuura, N. Shimizu, F. Hasegawa, and Y. Nannichi, Jpn. J. Appl. Phys. 23, L623 (1984)
4) J. A. Van Vechten, J. Appl. Phys. 53, 7082 (1982)
5) T. Fukuzawa, S. Semura, H. Saito, T. Ohta, Y. Uchida, and H. Nakashima, Appl. Phys. Lett. 45, 1 (1984)
6) H. Nakashima, S. Semura, T. Ohta, Y. Uchida, H. Saito, T. Fukuzawa, t. Kuroda, and K. L. I. Kobayashi, to be published in IEEE J. Quantum Electron. June issue
7) L. L. Chang and A. Koma, Appl. Phys. Lett. 29, 138 (1976)
8) P. M. Petroff, J. Vac. Sci. Technol. 14, 973 (1977)
9) R. M. Fleming, D. B. Mcwhan, A. C. Gossard W. Wiegmann, and R. A. Logan, J. Appl. Phys. 51, 357 (1980)
10) K. Ishida, T. Ohta, S. Semura, and H. Nakashima, to be submitted to Jpn. J. Appl. Phys.
11) J. W. Lee and W. P. Laidig, J. Electron. Materials, 13, 147 (1984)
12) H. C. Casey, Jr., and M. B. Panish, Phys. Rev. 162, 660 (1967)
13) H. Nakashima, T. Narusawa, S. Semura, and K. L. I. Kobayashi, Proc. 13th Int. Conf. Defect in Semicon. Coronad 1984 (Met. Soc. AIME. 1985) p.463
14) K. Meehan, N. Holonyak, Jr., J. M. Brown, N. A. Nixon, P. Gavrilovic, and R. D. Burnham, Appl. Phys. Lett. 45, 549 (1984)
15) M. E. Greiner and J. F. Gibbons, Appl. Phys. Lett. 44, 75 (1984)
16) T. Narusawa, Y. Uchida, K. L. I. Kobayashi, T. Ohta, M. Nakajima, and H. Nakashima, to be published in Proc. 11th Int. Symp. on GaAs and Related Compounds.
17) Y. Suzuki and H. Okamoto, J. Electron. Materials, 12, 397 (1983)
18) H. Yonezu, M. Ueno, T. Kamejima, and I. Hayashi, IEEE J. Quantum Electron. QE-15, 775 (1979)
19) Y. Suzuki, Y. Horikoshi, M. Kobayashi, and H. Okamoto, Electron. Lett. 20, 383 (1984)
20) S. Semura, T. Ohta, T. Kuroda, and H. Nakashima, to be submitted to Jpn. J. Appl. Phys.